Transactions on Electrical and Electronic Materials
https://doi.org/10.1007/s42341-020-00187-y

Online ISSN 2092-7592
Print ISSN 1229-7607

REGULAR PAPER

# Giant Dielectric Behaviour of Nb Modified CCTO Thin Film Prepared by Modified Sol–Gel Route

**A. K. Mishra[1] · D. Dwibedy[2] · M. Devi[1] · Manas R. Panigrahi[2]**

Received: 22 June 2019 / Revised: 14 January 2020 / Accepted: 14 February 2020


**Abstract**
Modified sol–gel technique has been used to prepare the Nb doped CCTO ceramic thin film. X-ray diffraction of the prepared film confirms the cubic perovskite structure of the material. The micrographs obtained from the Scanning Electron Microscope reveal plenty of rods like microstructure within the scan area. This is being reported for the first time in the studied film. Dielectric constant is measured with the frequency range 100 Hz–1 MHz and it is observed that, with increase in frequency the dielectric constant decreases. Further, it is also observed that, the rate of decrease of $\varepsilon_r$ with frequencies increases with increasing temperature. The dielectric loss of the material decreases with increasing frequency and at low frequency region the dielectric loss increases with increase in temperature. The studied material shows relaxor behaviour ($\gamma = 1.87$) and is confirmed by peaks broadening at low frequency with increasing temperature and the peaks shift to low frequency region with decreasing temperature. The broad band spectrum of high dielectric constant is seen over the studied temperature range. This relaxation behaviour arises due to space charge polarization. The absorption and transmittance nature of the film is also presented and the calculated value of energy band gap is found to be 2.52 eV.

**Keywords** Giant dielectric · Nb doped CCTO · Thin film · Band gap

## 1 Introduction

High dielectric constant materials have been attracting more attention by the researcher and scientist because of their versatile use and applications in and as different devices such as multi layer ceramic capacitors (MLCC), static random access memories (SRAM), dynamical random access memories (DRAM), ferroelectric random access memories (FRRAM) and many more. BT, PZT, PMNO etc. shows high dielectric constant and behave as normal (sharp Curie peak) or relaxor (diffused Curie peak) dielectric as seen from the graph of permittivity versus temperature. However, this high dielectric constant behaviour as a function of temperature is not desirable for many of the applications. $CaCu_3Ti_4O_{12}$, with massive dielectric permittivity of about 10,000 in a wider temperature range of 100–600 K has been discovered as a new lead free dielectric material [1–12]. When the material is probed with X-ray (high resolution) and neutron diffraction this material displays a reduction in 1 0 0 fold without any change in the crystallographic structure of long range order [13]. However, this extraordinary behaviour is also exhibited by the thin films of the material though the magnitude is lower [14–16].

During 1967 a particular compound of the family $ACu_3Ti_4O_{12}$ for A is Ca, Ba and Sr was discovered [17] and in 1979 their structure was determined [18]. $ACu_3Ti_4O_{12}$ oxide compound became important candidate which can produce higher dielectric constant and show perovskite structure which is complex and hence the material become a versatile candidate for different potential applications. Presently used materials viz. $BaTiO_3$ or relaxor ferroelectrics such as $Pb(Mg_{1/3}Nb_{2/3})O_3$[PMN], $Pb(Zn_{1/3}Nb_{2/3})O_3$ [PZN] and $Pb_{1-x}Lax(Zr_{1-y}Ti_y)O_3$ [PLZT] [19] are toxic because of the lead content, so not suitable for capacitor material as per green environment. So these are undesirable.

Transition of phases and unstability are the major problem with ferroelectric perovskite $BaTiO_3$. At high temperature $BaTiO_3$ is not suitable for use, the reason being its highly unstable and variation of dielectric constant with

✉ Manas R. Panigrahi
mrpanigrahi@vssut.ac.in

[1] Department of Physics, School of Applied Sciences, KIIT University, Bhubaneswar 751024, India

[2] Department of Physics, Veer Surendra Sai University of Technology, Burla, Sambalpur 768018, India

Published online: 23 February 2020

temperature. So, materials that exhibit phase transition near Curie temperature and produce high dielectric constant are not the suitable material for device application. So, on the other hand, $CaCu_3Ti_4O_{12}$ a high dielectric constant material discovered by Subramanian et al. belonging to the family of $ACu_3Ti_4O_{12}$, during 2000 [20] is the best choice so far. $CaCu_3Ti_4O_{12}$ exhibit a pseudo cubic perovskite structure with lattice vector 7.391 Å and falls under space group of Im3 [21]. CCTO exhibit high dielectric constant of the range 10,000 and is observed to be steady in the temperature range 100–600 K. This property helps the material to find a prominent position in many industrial applications basically in the field of microelectronics and memory devices. This is because the level of miniaturization of a material depends on its static dielectric constant. This makes the material a promising candidate for various industrial revolutions. It has potential applications in the electronic industries for the manufacturing of multilayer ceramic capacitors (MLCC), devices for microwave, electronic kits for automobile industries and aircrafts, random access memory (RAMs), etc. [22, 23]. Though a lot of work has been done both in the field of theoretical and experimental research to know the origin of giant dielectric constant behaviour of $CaCu_3Ti_4O_{12}$ still it need discussions and dialogue and hence there are scopes to solve. Out of the many theories the one that is well accepted by the researchers is IBLC i.e. internal grain boundary barrier layer capacitance model [24].

Though several works have been reported on dielectric properties of both single crystal CCTO and poly crystalline CCTO ceramics, the high dielectric loss of the material which of the order of $> 0.05$ at 1 kHz is a fascinating problem for some applications based on capacitive component. Thus, there is a requirement for the development of a lead free material having high dielectric constant and low dielectric loss with better stability in a wider frequency and temperature range.

Presently, several researchers reported different synthesis techniques for fabrication of this material for its giant dielectric properties [25–27]. Out of these techniques, the solid state reaction method is conventional and heavily adopted has some demerits in sense of maintaining the homogeneity of the starting material. So, to get a single phase longer sintering time and higher sintering temperature are required for solid state diffusion to take place. Therefore, for good homogeneity a suitable chemical method is necessary with lower processing temperature and processing time which can save both energy and time. In this paper, modified sol–gel process as a preparation tool is reported for better morphology, and dielectric constant. Now it is high time to understand the influence of the participating material and different processing parameters to get better and optimized properties for the modified CCTO film. The dielectric behaviour at a different range of temperature and frequencies are mentioned here.

Studies on ideal material and their isomorphs for dielectric properties gained considerable attention and importance for miniaturization of capacitors and other electronic devices. Dielectric materials which can exhibit high dielectric permittivity with very low dielectric loss have always been in demand in science and technology. Importance are also given for better ideas and design with high efficiency for the material to be used in structures and microwave devices. Best suited materials and synthesis technique are choosen for the development of new type ceramic dielectric materials. Materials showing high dielectric permittivity have gained considerable attention. There have been continuous effort since 1921 after the discovery of ferro-electricity in Rochelle salt for new material which can show high dielectric ($\varepsilon_r$). The key issue for the development of ceramic capacitor technology (CCT) is the hot demand of ceramic based capacitors having higher dielectric permittivity. But, there was not much advancement in the achievement of high $\varepsilon_r$ dielectric materials till the dielectric constant of $BaTiO_3$ was discovered by Thurnauer as $\varepsilon_r = 1100$ in 1941. But, there is some limitation of applications of $BaTiO_3$ as the dielectric constant is strongly temperature dependent [28]. Keeping this in view researchers and technologist have seriously worked to obtain an alternative which can show thermally stable high $\varepsilon_r$ in the wider frequency and temperature range. The studied perovskites oxides have exhibited the above stated properties in the studied range of frequency and temperature i.e. frequency varies from 1 kHz–1 MHz and temperature varies from 100 to 600 K.

## 2 Materials and Methods

Nb-doped CCTO ($Nb_xCCTO_{1-x}$) thin film for $x = 0.04$ have been prepared by the modified sol–gel method. The interacting reagent materials were $CaCO_3$ (Merck 99.99% pure), $Cu_2O$ (Merck 99.99% pure), $TiO_2$ (Merck 99.99% pure) and $Nb_2O_5$ (Merck 99.99% pure). Powders of the starting reagent materials were mixed with stoichiometric proportion and a particular quantity of acetic acid was added to get smooth and uniform paste. Thereafter, deionised water was added drop by drop and the solution was stirred using magnetic stirrer continuously at room temperature until a transparent homogeneous sol is formed. Then, to the sol 0.1 M $HNO_3$ was added. Then for refluxing the sample was subjected at 180 °C for 6–7 h. Finally, the material was prepared in gel form and it was then kept for a day. Next day using doctor's blade method Nb- doped CCTO thin film was deposited on the ITO glass slide. Then the prepared film was annealed 200 °C and was then subjected to characterization. X-ray diffracton (XRD, Shimandzu-6100) with CuKα radiation ($\lambda = .1540$ nm) had been used to analyse the crystal structure of the prepared film. For morphological studies

the sample was subjected to scanning electron microscope (Hitachi SU3500) and EDX analysis was done with Oxford X-act Penta FET precision attached to the above SEM. For dielectric measurement Hioki LCR meter was used and the data were recorded at a gap of 5 °C. UV–Vis spectrometer (UV3092) has been used for the measurement of optical transmittance spectra of the prepared film in the wavelength range 300–850 nm with spectral band width 5 nm. The scanning was done at an interval of 2 nm with medium speed (Fig. 1).

## 3 Result and discussion

### 3.1 Structure

Figure 2 shows the room temperature XRD patterns of $CaCu_3Ti_4O_{12}$ (CCTO) and Nb doped $CaCu_3Ti_4O_{12}$ (CCTO-Nb) thin films. The material crystallizes in cubic perovskite structure. For the 100% RI peak the crystallite size of the identified crystalline phase are calculated using the corrected form of well known Debye–Scherrer equation given as

$$D_{hkl} = \frac{K\lambda}{\beta' \cos\theta} \tag{1}$$

where $\beta' = (L - l)$ = full width at half maximum (FWHM), L = the line width, l = the instrumental broadening, K represents the shape factor and is equal to 0.9, $\theta$ is the glancing angle and λ = wave length of Cu $K_\alpha$ = 1.5406 Å.

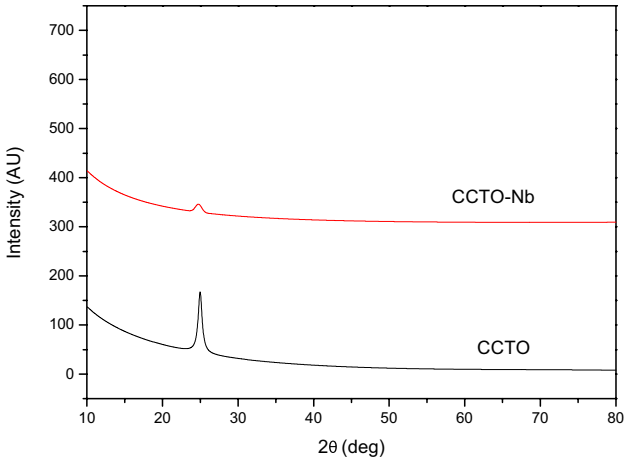


**Fig. 2** X-ray diffractogram of CCTO and CCTO-Nb thin films

The instrumental broadening can be calculated using Eq. 2 as follows,

$$b = \left[\frac{2\Delta\lambda}{\lambda} \tan\left(\frac{2\theta}{2}\right)\right] + \left[arc\ \tan\frac{W_R}{R_G}\right] \tag{2}$$

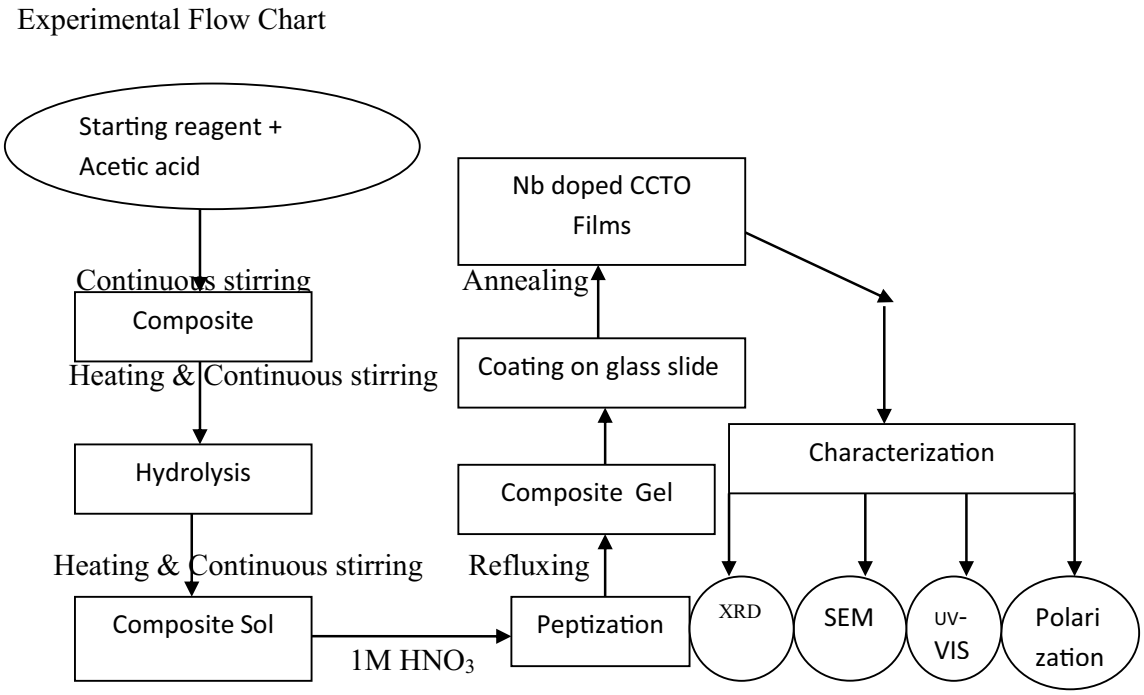


**Fig. 1** Experimental flow chart

where $\frac{\Delta\lambda}{\lambda}$ = the resolution of diffractometer = $2.5 \times 10^{-3}$, $\theta$ is the Bragg angle, $W_R$ = width of the receiving slit = 1 mm and $R_G$ = the goniometer radius (200 mm).

The presence of sharp peaks of variable intensity in the XRD pattern confirms the formation of single phase material with little trace phase. From XRD it is clear that sample have perovskite major phase. The different structural parameters of the synthesized samples are presented in Table 1 after refinement using whole profile fitting method. Finally, unit cell was selected on the basis of good agreement between observed (obs) and calculated (cal) inter planar spacing d (i.e., $\Sigma\Delta d = \Sigma (d_{obs} - d_{cal})$ = minimum) of the peaks. The refined parameters are also presented in Table 1. The unit cell parameters of Nb doped CCTO thin film as obtained after refinement are a = b=c = 8.7 Å and unit cell volume is 658.5 $Å^3$. Crystallite size is estimated to be 95.96 Å with micro strain 1.58 and integral breadth 1.536 Å for Nb doped CCTO thin film.

## 3.2 Microstructure

Figure 3 shows the Scanning Electron Microscopic microstructure of CCTO Fig. 3a and Nb modified CCTO Fig. 3b. As seen, morphology is observed to be very dense without any impurity phase. The microstructure is very interesting as the virgin CCTO has shown a bead like morphology grown to rod like structure which are available in bundles in Nb doped CCTO thin film. This type of microstructure in the studied material is yet to be reported. This type of microstructure may be due to the transport phenomena of Nb towards A site. The off valent niobium element may be marging into the Cu region and enhancing the grain growth due to the ability of segregated Nb ion to produce bundles of cable (rod) like structures. This may be one of the reason for giant dielectric behaviour of Nb doped CCTO thin film. Figure 4 shows the EDX spectrum of Nb modified CCTO thin film. Presences of participating elements are confirmed from the spectrum. The elemental composition shows the singular phase behaviour of the material and are presented in Table 2.

**Table 1** Structural data of CCTO and CCTO-Nb Thin film

| sample | Position (2θ) | d-spacing (Å) | FWHM | Microstrain (%) | Crystallite size (nm) | Integral Breadth (Å) | Area | Lattice strain |
|---|---|---|---|---|---|---|---|---|
| CCTO | 24.978 | 3.562 | 0.384 | 0.51 | 21.186 | 0.972 | 68.798 | |
| CCTO-Nb | 24.770 | 3.592 | 1.152 | 2.07 | 07.062 | 1.045 | 23.139 | − 0.008 |

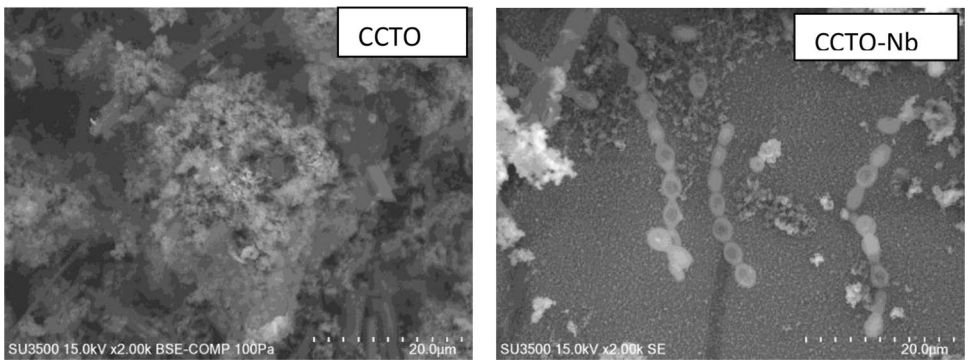


**Fig. 3** SEM morphology of CCTO and CCTO-Nb thin films

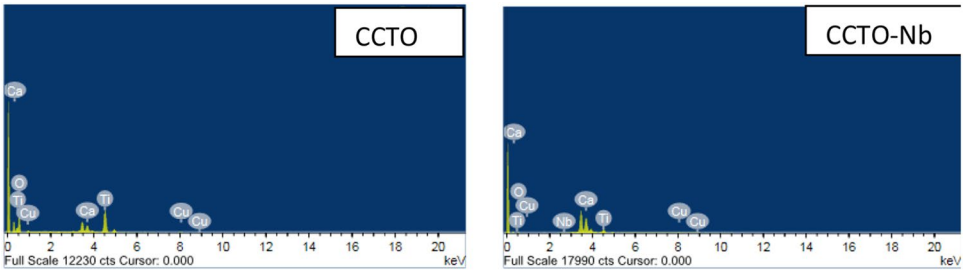


**Fig. 4** EDX spectrum of CCTO and CCTO-Nb thin films

**Table 2** Compositional analysis of CCTO-Nb thin film

| Element | Experimental wt% | Theoretical wt% |
|---|---|---|
| O | 16.23 | 18.74 |
| Ca | 4.52 | 4.02 |
| Ti | 4.50 | 3.98 |
| Cu | 74.62 | 72.08 |
| Nb | 0.14 | 1.18 |
| Total | 100 | 100 |

The variation of dielectric permittivity of the prepared material with temperature at various frequency levels ranging from 100 Hz to 1 MHz is shown in Fig. 5. It is seen that, the dielectric permittivity decreases with increase in frequency and at the same time it increases with increase in temperatures. This is a typical behaviour of the dielectric material. The dielectric permittivity increases slowly and attains a maximum value of 97,635 at 324.23 °C for 1 kHz frequency. This is the obvious nature of all dielectric materials to have relatively high dielectric constant at low frequencies. It is seen that with increase in frequency the dielectric permittivity decreases. This may be attributed to the fact that at high frequency dipoles cannot follow the applied field. This may also be attributed to the decrease of total polarization which arises out of dipoles and trapped charge carriers. Trapped charge carriers contribute to the total polarization in most of the materials in general and in polymer in particular because polymer systems contain a large number of trapping sites. So, it is expected that trapped charge carriers plays a major role in the larger dielectric values at lower frequencies. With increase in the applied field frequency dipoles hardly orient themselves in the direction of applied field. Thus, the value of dielectric permittivity decreases at higher frequencies. Here it is seen that, with increase in temperature dielectric permittivity increases and it decreases after $T_c$ with increase in temperature. It is observed that with increase in frequency the dielectric permittivity of the prepared material decreases in the studied range of frequency i.e. from 100 Hz to 1 MHz. The dielectric constant of the system decreases with the increasing frequency in the investigated range of (100 Hz–1 MHz). A relaxation of the dielectric constant gives some hints that the studied material is somewhat of relaxor nature.

The high dielectric constant may also be due to the soft mode character of optical phonon spectrum in the polar region. This reinforce the hypothesis of soft mode character that, the relatively giant dielectric behaviour of CCTO and its modified compound is due to soft mode nature of the material. However, Maxwell–Wagner effect hide this behaviour.

The variation of dielectric loss of the prepared material with temperature at various frequency levels ranging from 100 Hz to 1 MHz is shown in Fig. 6. The value of dielectric loss is lower for higher temperature and increasing with frequency for lower value of temperature. The values of the dielectric permittivity and tan δ were observed to be strongly frequency-dependent. From the variation of tan δ with temperature at different frequency, it is seen that the values of the tangent loss (tan δ) increases with increasing frequency, indicating a normal behavior of dielectrics. But, with increase of temperature, the nature of variation shows the existence of tan δ peak at a higher frequency. As frequencies increases the loss value also increases but after Tm, tan δ becomes closer in all frequencies. The same type of relaxation of the loss is yet another signature that the material is closer to the diffuse phase transition. Dielectric loss of a material is the dissipation of electrical energy in

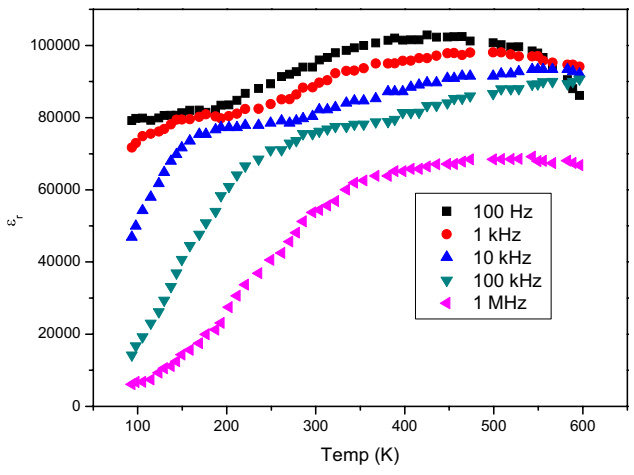


**Fig. 5** Dielectric constant vs. temperature at different frequencies of CCTO-Nb thin film

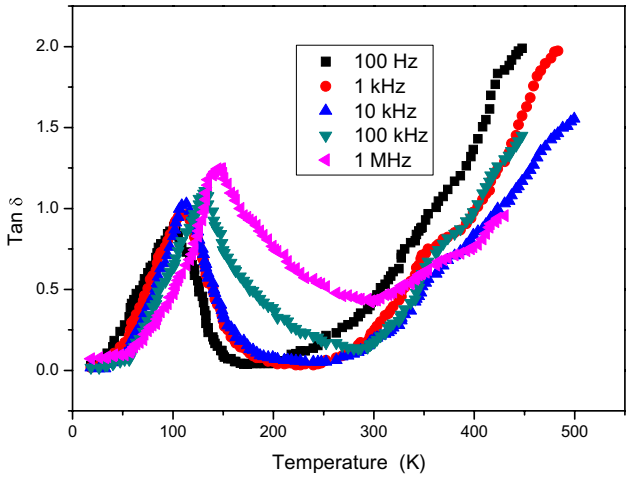


**Fig. 6** Dielectric loss vs. temperature at different frequencies of CCTO-Nb thin film

a quantitative way. This dissipation of energy may be due to different physical processes like, electrical conduction, dielectric relaxation, dielectric resonance and loss from non-linear processes. This may also be attributed due to delay between the electric field and electric displacement vector. The net dielectric loss of a material stands due to the sum total of intrinsic and extrinsic losses. The intrinsic losses depend on the crystal structure and can be explained as the interaction of phonon with the electric field (ac), since, the equilibrium of the phonon system is altered due to the field and hence relaxation can be explained as energy dissipation. The phonon frequency is much higher than the microwave frequency and thus the sample get heated up as the energy of the field dissipated heat. So, intrinsic losses are due to crystal symmetry, frequency of the field and temperature. Intrinsic losses fix the lower limit of the losses in the defect free crystal. Additionally, extrinsic losses are due to imperfections in the crystal lattice. Thus extrinsic losses may be attributed to one or all of the following; impurities, microstructural defects, grain boundaries, porosity, microcracks, order–disorder, random crystallite orientation, dislocations, vacancies, dopant atoms etc. Thus, it is established that extrinsic losses are due to lattice defects. Thus, the extrinsic losses can be reduced to a minimum by proper material processing.

Furthermore, the high loss may be due to the overlapping of the electron clouds caused by the lattice shrinkage of this superlattice. The dielectric loss peak indicates the existence of a polarizing species with a comparatively lengthy relaxation time in the super lattice. The variation of the dielectric loss peak may be due to the variation in tailing of the dielectric loss peak and may also be attributed to the variation in the periodicity of the superlattices.

Very high electric fields can free electrons from atoms, and accelerate them to such high energies that they can, in turn, free other electrons, in an avalanche process (or electrical discharge). This is called dielectric breakdown, and the field necessary to start this is called the dielectric strength or breakdown strength. The breakdown field vs current density (Fig. 7) behaviour of the CCTO and CCTO-Nb films are presented in the above mentioned graph. The current range is from 0.5 to 300 micro ampere. Dielectric strength refers to the ability of an insulating material to resist the utmost voltage imposed on it for a long duration without failure, the voltage at which failure occurs is known as Breakdown Voltage. The failure of an insulator is the loss of the insulator to its electric insulation property and its transformation into conductor, the maximum electric field applied on the insulator at which failure occurs is called dielectric strength.

The inverse dielectric constant versus temperature graph is shown in Fig. 8. Figure 9 represents the graph between reduced dielectric constant $\left(\frac{\varepsilon}{\varepsilon_m}\right)$ versus reduced temperature ($\tau$) at various frequencies for the better illustration of phase transition broadening. There is a little dispersion of the full width of the dielectric spectrum over a wider frequency range as seen in other type of relaxor materials. This is yet another illustration to see the relaxor nature of the studied material.

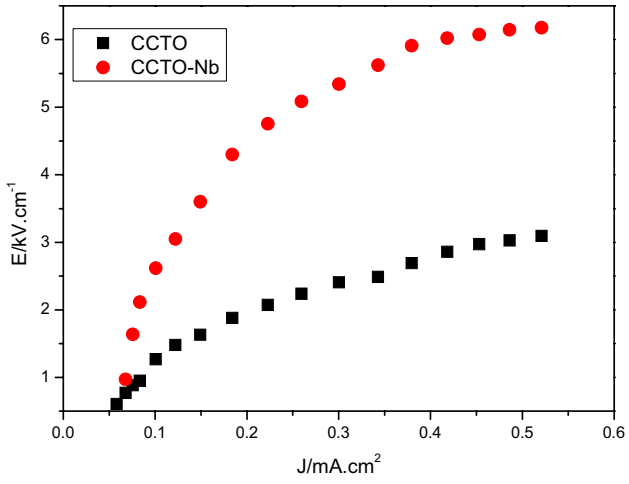


**Fig. 7** Breakdown field vs current density of CCTO and CCTO-Nb thin film

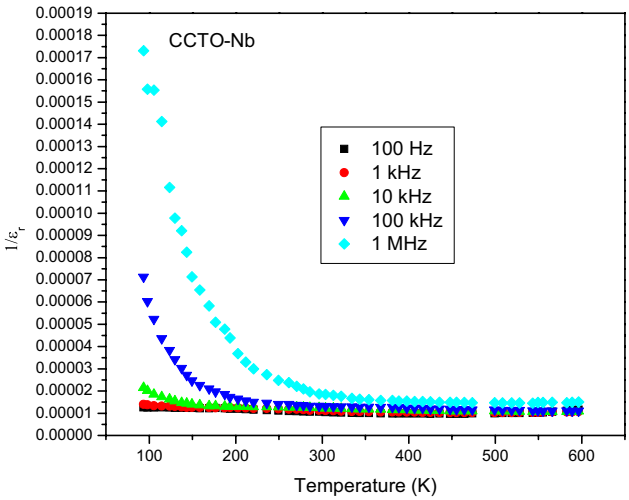


**Fig. 8** Inverse dielectric constant vs. temperature at different frequencies of CCTO-Nb thin film

The well known modified Curie–Weiss Eq. (3) represents the deviation from normal Curie–Weiss behaviour for ferroelectric- paraelectric phase transition of the widened naute of the material as follows [26–28],

$$\frac{1}{\varepsilon}-\frac{1}{\varepsilon_m}=\frac{(T-T_m)^{\gamma}}{C} \tag{3}$$

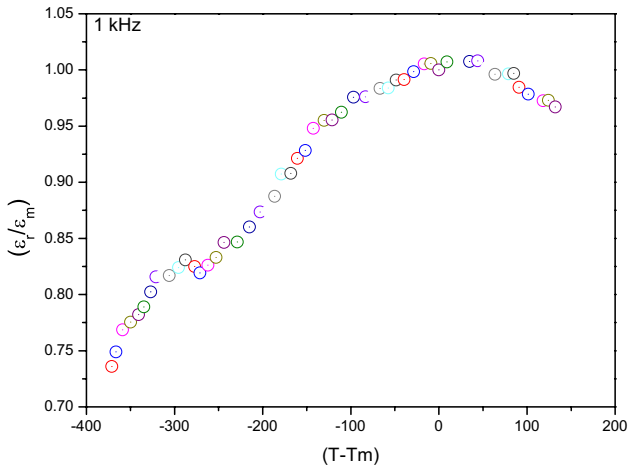


**Fig. 9** Reduced dielectric constant vs. reduced temperature of CCTO-Nb thin film at 1 kHz

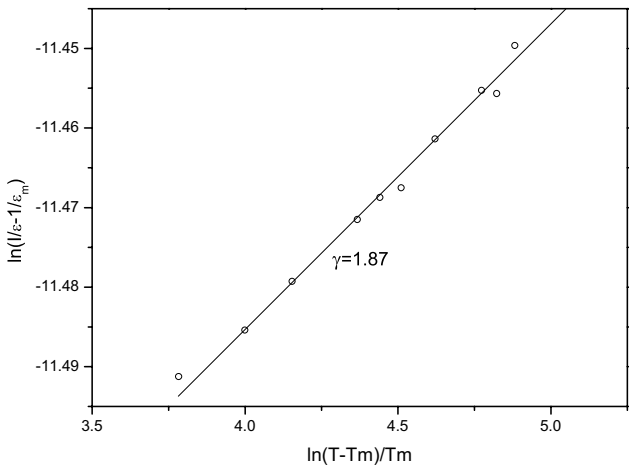


**Fig. 10** G plot of CCTO-Nb thin film at 1 kHz

where γ gives the degree of phase transition and is a constant. For γ = 1, it is normal phase transition and follow normal Curie–Weiss law and when γ > 1 it represents a diffuse phase transition. C is also a constant [29].

A graph between $\ln(1/\varepsilon - 1/\varepsilon_m)$ versus. $\ln(T - T_m)$ is shown in Fig. 10. Here the γ value is estimated to be 1.87 at 1 kHz frequency and is presented in Table 3. This shows that there is a clear diffuse phase transition. This nature of diffuse phase transition and deviation from normal Curie–Weiss behaviour can be attributed to disordering. When there is a structural disordering in the cationic arrangement in one or more crystallographic sites of the structure, there occurs compositional fluctuations and hence diffusiveness occurs. In the relaxation process the orientational polarization plays a major role. Another parameter which will describe the degree of relaxation nature of the material in the frequency range 1–100 kHz is given by Eq. (4) [30],

$$\Delta T_{Relax} = T\varepsilon_m(100\ \text{kHz}) - T\varepsilon_m(1\ \text{kHz}) \tag{4}$$

For the studied sample the estimated value of $\Delta T_{relax}$ is 2.32 K. It is observed that Nb doped $CaCu_3Ti_4O_{12}$ (Nb-CCTO) thin film follows Curie–Weiss law at temperature higher than $T_m$. This is based on Curie–Weiss law based Characterization and different derived empirical parameters like $\Delta T_m$, γ, and $\Delta T_{relax}$. Based on the above facts, i.e. large deviation from the Curie–Weiss type behavior, the value of relaxation temperature $\Delta T_{relax} = 2.32$ K, and $\gamma = 1.87$, confirms the relaxor nature of Nb doped $CaCu_3Ti_4O_{12}$(CCTO-Nb) thin film.

Figure 11 shows the Vogel–Fulture relation of the material for the estimation of the activation energy ($E_a$) and is represented by the relation,

$$f = f_0 \exp\left[\frac{-E_a}{k_B(T_m - T_f)}\right], \tag{5}$$

where $f_0$ = attempt frequency, $E_a$ = average activation energy, $k_B$ = Boltzman constant, $T_f$ = freezing temperature of polarization fluctuation and $f_0$ = the pre exponential factor. The different fitting parameters for the compound are found to be, $E_a = 0.111$ eV, $T_f = 99.6$ K, $f_0 = 100.04 \times 10$ Hz.

In the para-electric phase the average value of activation energy is observed to be very low. In many such ferroelectric compound low value of activation energy has been observed. This may be because of the availability of less number of mobile ions in the ionic solids and these ions might have been trapped in relatively stable potential well when they begins to move through the solid. When temperature rises the donor cations play a major role in the conduction process. These cations create band much nearer to the conduction band called donor-level band. Thus, to activate the donors a small amount of energy is necessary. Additionally, a large number of donors or acceptors can be created by slightly changing the stoichiometry of multi metal complex oxides (MMCO), which in turn creates acceptors or donors like states in the vicinity of conduction or the valence bands and to activate these donors or acceptors small amount of energy is required.

**Table 3** Empirical dielectric data of CCTO-Nb thin film

| Sample | Parameters | | | | | |
|---|---|---|---|---|---|---|
| | $\varepsilon_m$ | $T_m$ (K) | $T_o$ (K) | $T_{cw}$ (K) | $\Delta T_m$ (K) | γ |
| CCTO-Nb | 97,635 | 455.39 | 123.2 | 260.93 | 26.86 | 1.87 |

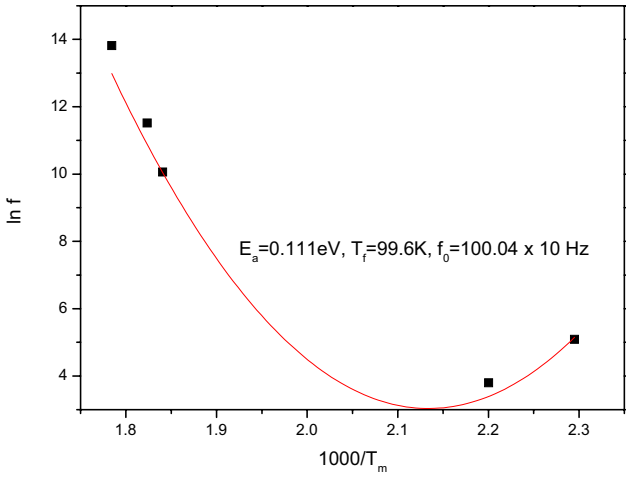


**Fig. 11** V-F relation of CCTO-Nb thin film at 1 kHz

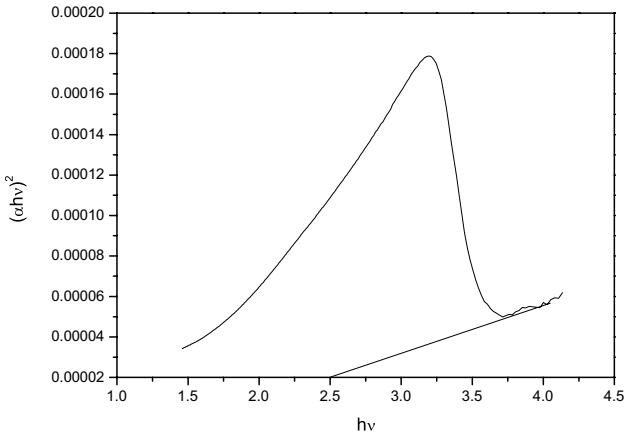


**Fig. 12** Band gap of Nb doped CCTO thin film

Figure 12 represents the band gap of Nb doped CCTO thin film in the studied composition. From the graph of (hν) i.e. incident photon energy vs. $(\alpha h\nu)^m$, the value of band gap can be estimated. From the graph the value of energy band gap is calculated to be 2.52 eV. The values of m varies depending on the electronic transition type. Electronic transition is strong for direct band gap semiconductor. This is because electronic transition from valence band to conduction band is electrical dipole allowed, whereas valence band to conduction band electronic transition is electrical dipole forbidden in indirect band gap semiconductor and the transition is phonon assisted.

## 4 Conclusion

Here in this present article the structure and properties of dielectric of Nb doped $CaCu_3Ti_4O_{12}$(CCTO-Nb) thin film is discussed. The materials were synthesized by modified sol–gel route. The structure of this material is observed to be cubic. The dielectric constant and ($\varepsilon$) and dielectric loss (tan $\delta$) of Nb doped $CaCu_3Ti_4O_{12}$(CCTO-Nb) film with variation of temperature (50–500 K) and variation of frequencies (100 Hz–1 MHz) suggest that the synthesized material shows diffuse phase transition behaviour with giant dielectric constant. The maximum relative permittivity of the materials was very high i.e. (≈96,635 at 1 kHz). The tangent loss value decreases to a lower value with increase in temperature and then further increases at the proximity of the highest temperature for almost all frequencies. This may attribute to the fact that, delocalization of electron of the bulk materials takes place through Cu sub lattice. $Cu^{2+}$ captured the extra electron to get converted to $Cu^+$ cations and in this process of electron transfer Ti plays the role of a mediator. This may be due to the highly distorted structure of the coumpound. Furthermore, the insulating nature of the material could be explained in the light that the presence of Ti cations in the Copper site does not allow the electron transfer between the $Cu^+$ and $Cu^{2+}$ cations at the A-site. From the absorption data the optical band gap value of the material is estimated to be 2.52 eV.

## References


1. A. Deschanvres, B. Raveau, F. Tollemer, Bull. Soc. Chim. Fr. **11**, 4077 (1967)
2. B. Bochu, M.N. Deschizeaux, J.C. Joubert et al., Solid State Chem. **29**, 291 (1979)
3. A.J. Moulson, J.M. Herbert, *Electroceramics*, 2nd edn. (Wiley, Chichester, 2003)
4. L.C. Kretly, J.M. Sasaki, A.S.B. Sombra et al., Microw. Opt. Technol. Lett. **39**, 145 (2003)
5. P. Jha, P. Arora, A.K. Ganguli, Mater. Lett. **57**, 2443 (2003)
6. S. Jin, H. Xia, Y. Zhang, J. Guo, J. Xu, Mater. Lett. **61**, 1404 (2007)
7. H. Liu, H. Yu, D. Lou, M. Cao, J. Mater. Process. Technol. **208**, 145 (2008)
8. L. Wu, Y. Zhu, S. Park, S. Shapiro et al., Phys. Rev. B **71**, 014118 (2005)
9. M.A. Subramanian, M.H. Whangbo, Chem. Mater. **18**, 3257 (2006)
10. C.P. Liu, T.T. Fang, Chem. Mater. **17**, 5167 (2005)
11. A.V. Pronin, A.I. Ritus, A.A. Volkov et al., Phys. Rev. B **66**, 052105 (2002)
12. R. Fichtl, S.G. Ebbinghaus, A. Loidl, P. Lunkenheimer, Phys. Rev. B **70**, 172102 (2004)
13. L. Singh, K.D. Mandal, U.S. Rai, Mater. Res. Bull. **48**, 2117 (2013)
14. M.A. Subramanian, W.J. Marshall, T.G. Calvarese, A.W. Sleight, J. Phys. Chem. Solids **64**, 1569 (2003)
15. M. Ibrahim, M. Ikhwan, S.D. Hutagalung, Z.A. Ahmad, Mater. Chem. Phys. **112**, 83 (2008)
16. L. Singh et al., Prog. Cryst. Growth Charact. Mater. **60**, 15 (2014)
17. C. Mu, H. Zhang, Y. He, P. Liu, J. Shen, Mater. Sci. Eng., B **162**, 195 (2009)
18. K.D. Mandal, L. Singh, S. Sharma, U.S. Rai, M.M. Singh, J. Sol-Gel. Sci. Technol. **66**, 50 (2013)

19. N.B. Singh, M. Gillan, D. Arnold, R. Yanamaddi, J. Emerg. Mater **2**, 1 (2013)
20. S.F. Shao, P. Zheng, C.L. Wang, J.C. Li, M.L. Zhao, Appl. Phys. Lett. **91**, 042905 (2007)
21. S.H. Hong, S.W. Choi, J. Am. Ceram. Soc. **90**, 4009 (2007)
22. K.D. Mandal, A.K. Rai, L. Singh, O. Prakash, Bull. Mater. Sci. **35**, 433 (2012)
23. L.Y. Ooi, Z.A. Ahmad, S.D. Hutagalung, J. Alloys Compd. **476**, 477 (2009)
24. K.D. Mandal, D. Kumar, A.K. Rai, O. Prakash, Mater. Chem. Phys. **122**, 217 (2010)
25. K.D. Mandal, D. Kumar, A.K. Rai, O. Prakash, J. Alloys Compd. **491**, 507 (2010)
26. N.B. Singh, D. Knuteson, D. Kahler, M. House, B. Wagner, M. King, Ceram. Trans. **235**, 65 (2012)
27. A. Sen, U.N. Maiti, R. Thapa, K.K. Chattopadhyay, J. Alloys Compd. **506**, 853 (2010)
28. M. Li, G. Cai, D.F. Zhang, W.Y. Wang, W.J. Wang, X.L. Chen, J. Appl. Phys. **104**, 074107 (2008)
29. B. Jaffe, J.W.R. Cook, H. Jaffe, *Piezoelectric Ceramics* (Academic Press, New York, 1971)
30. J.M. Xue, J. Wang, T.M. Rao, J. Am. Ceram. Soc. **84**(3), 660 (2001)